Front. Agr. Sci. Eng. 2019, **6**(2): 172–180
https://doi.org/10.15302/J-FASE-2019256
Available online at http://journal.hep.com.cn/fase

RESEARCH ARTICLE

Detection of Huanglongbing (citrus greening) based on hyperspectral image analysis and PCR

Kejian WANG[1,2], Dongmei GUO[3], Yao ZHANG[4], Lie DENG[1], Rangjin XIE[1], Qiang LV[1], Shilai YI[1], Yongqiang ZHENG[1], Yanyan MA[1], Shaolan HE (✉)[1]

1 Southwest University/Citrus Research Institute of Chinese Academy of Agricultural Sciences, Chongqing 400712, China
2 National Agricultural Technology Extension and Service Center, Beijing 100125, China
3 Chengdu Plant Quarantine Station, Chengdu 610000, China
4 Key Laboratory of Modern Precision Agriculture System Integration Research, China Agricultural University, Beijing 100083, China

Abstract Huanglongbing (HLB, citrus greening) is one of the most serious quarantine diseases of citrus worldwide. To monitor in real-time, recognize diseased trees, and efficiently prevent and control HLB disease in citrus, it is necessary to develop a rapid diagnostic method to detect HLB infected plants without symptoms. This study used Newhall navel orange plants as the research subject, and collected normal color leaf samples and chlorotic leaf samples from a healthy orchard and an HLB-infected orchard, respectively. First, hyperspectral data of the upper and lower leaf surfaces were obtained, and then the polymerase chain reaction (PCR) was used to detect the HLB bacterium in each leaf. The PCR test results showed that all samples from the healthy orchard were negative, and a portion of the samples from the infected orchard were positive. According to these results, the leaf samples from the orchards were divided into disease-free leaves and HLB-positive leaves, and the least squares support vector machine recognition model was established based on the leaf hyperspectral reflectance. The effect on the model of the spectra obtained from the upper and lower leaf surfaces was investigated and different pretreatment methods were compared and analyzed. It was observed that the HLB recognition rate values of the calibration and validation sets based on upper leaf surface spectra under 9-point smoothing pretreatment were 100% and 92.5%, respectively. The recognition rate values based on lower leaf surface spectra under the second-order derivative pretreatment were also 100% and 92.5%, respectively. Both upper and lower leaf surface spectra were available for recognition of HLB-infected leaves, and the HLB PCR-positive leaves could be distinguished from the healthy by the hyperspectral modeling analysis. The results of this study show that early and nondestructive detection of HLB-infected leaves without symptoms is possible, which provides a basis for the hyperspectral diagnosis of citrus with HLB.

Keywords citrus, HLB, hyperspectral, identification, PCR

1 Introduction

Huanglongbing (HLB, citrus greening) is a quarantinable disease of citrus around the world. HLB has a history of more than 100 years, and is impacting the global citrus industry with increasing severity. After infection with HLB, the vigor of citrus trees gradually declines, the fruit set decreases and the production of fruits falls sharply. The fruit becomes smaller with abnormal color commonly known as "red fruit," and lose nutritional value. When the whole plant is infected, there is almost no yield, and finally the tree will die[1]. So far, there is no effective treatment for HLB disease. Therefore, real-time identification and removal of the infected plants is the most important and effective prevention and control measures.

Until recently, identification of HLB has been based on appearance of symptoms. Now polymerase chain reaction (PCR) tests have been developed that can rapid and accurately identify pre-symptomatic HLB infection. However, identification of symptoms in the field is limited by the knowledge and experience of the inspectors, and then only by skilled inspectors when symptoms become obvious. Molecular identification based on PCR technology is costly and takes longer. Therefore, it is important to develop accurate, efficient and real-time detection technology for HLB. Real-time and high-efficiency detection of

Received March 12, 2018; accepted March 14, 2019

Correspondence: heshaolan@cric.cn

the infected plants before symptoms develop would be of great significance for the prevention and control for HLB disease. Near infrared (NIR) spectroscopy is a modern analytical technology with the advantage of being a simple, rapid and nondestructive means of inspection. Compared with the multispectral information, the hyperspectral analysis technique developed in recent years has higher spectral resolution, which can detect subtle changes in the spectral information from the sample, and detect the external sample features. With the rapid development of hyperspectral remote sensing technology, hyperspectral imaging technology used for the diagnosis of crop diseases has become a key area of research. Hyperspectral imaging technology combined with modern modeling and data analysis techniques can accurately identify the internal properties and external features of a test object and may identify a disease before symptoms appear. Therefore, it offers a great advantage for the early identification of plant disease.

In recent years, many scientists have studied the use of multi-spectral and hyperspectral analysis technology to diagnose diseases of crops, such as wheat[2,3], rice[4,5], Chinese cabbage[6], tomato, eggplant[7,8], cucumber[9], soybean[10,11] and cotton[12,13]. It has also been applied to some diseases of trees, such as apple, chestnut, and *Pinus massoniana*. The spectral detection and ground-based remote sensing technology for citrus HLB disease are also receiving considerable attention. Sankaran et al.[14] identified healthy leaves and HLB-infected leaves using linear discriminant analysis, Quadratic discriminant analysis (QDA), K-nearest neighbor, and soft independent modeling class analog classification. The results showed that recognition using the second-order derivative spectra combined with QDA was the best with an overall classification accuracy of up to 95%. The Citrus Research Center at the University of Florida also established a recognition model of HLB disease based on aerial remote sensing and multi-spectral technology[15,16]. Mei et al.[17] and Deng et al.[18,19] studied early nondestructive detection and diagnosis of citrus HLB disease based on hyperspectral imaging. These studies showed the advantages and value of spectroscopy applied to the identification of HLB disease, and also provided a reference for the development of identification technology for HLB disease. However, the above studies mostly established models used citrus samples with symptoms of HLB, but gave little consideration to asymptomatic samples. In this study, two kinds of samples, normal leaves (asymptomatic), and chlorotic leaves (symptomatic) from orchards were collected, and hyperspectral images of the upper and lower leaf surfaces were taken. Based on PCR results for all the leaf samples, the leaves were divided into two types: HLB-negative leaves and HLB-positive leaves. Two kinds of models to identify citrus with and without HLB were established, and a new method is proposed for the simultaneously identification of asymptomatic and symptomatic leaves, which could provide the basis for the rapid diagnosis of citrus HLB disease.

2 Materials and methods

2.1 Materials

Experiments were conducted using leaves collected from citrus orchards in Xunwu County in Jiangxi Province on 11 October 2015. Ten- to 13-year-old naval orange trees (*Citrus sinensis* cv. Newhall) on trifoliate orange (*Poncirus trifoliata*) rootstocks were sampled. Leaves were collected from orchards with and without HLB symptoms. Forty trees with varying severity of disease were selected in the HLB-infected orchard. Eight to 12 leaves were collected from each tree to give a total of 400 leaves; 200 leaves of normal color and 200 leaves with varying degrees of yellowing. Twenty trees including visually healthy plants and those with suspected nitrogen deficiency were chosen in the orchard without HLB symptoms. Eight to 12 leaves were collected from each tree to give a total of 200 leaves; 100 leaves with normal color and 100 chlorotic leaves. The samples were transported in a cooler to the laboratory with minimal delay, where the samples were cleaned and numbered, and hyperspectral imaging and PCR testing conducted.

2.2 Acquisition of leaf hyperspectral images

A hyperspectral imaging system was used to acquire the hyperspectral data in a dark box as shown in Fig. 1. The hyperspectral imaging system consisted of the following parts[20]: (1) hyperspectral spectrometer (ImSpector, V10E, Specim, Spectral Imaging Ltd. Oulu, Finland), (2) EMCCD camera (Raptor photonics, Inc., FA285-CL, Antrim, Northern Ireland), (3) light source (150 W/21 V halogen tungsten lamp, Illumination Technologies, Inc., East Syracuse, NY, USA), (4) motion controller, and (5) computer. The spectral range is 400–1000 nm, and the spatial resolution is 2.8 mm.

The hyperspectral imaging system was turned on for preheating for about half an hour before testing. The camera height was set according to the imaging definition. The parameters were set as follows. The distance between camera lens and movable platform was 400 mm. The exposure time was 60 ms. The speed of the movable platform was 1.87 mm·s^{-1}. To reduce the effect of temperature on spectral reflectance, laboratory temperature was maintained at 20°C, the samples were numbered and placed on the platform, and the hyperspectral images of the leaf sample were taken from both upper and lower surfaces. Then the calibrated hyperspectral images were obtained based on the following equation:

$$R = (R_S - R_D)/(R_W - R_D)$$

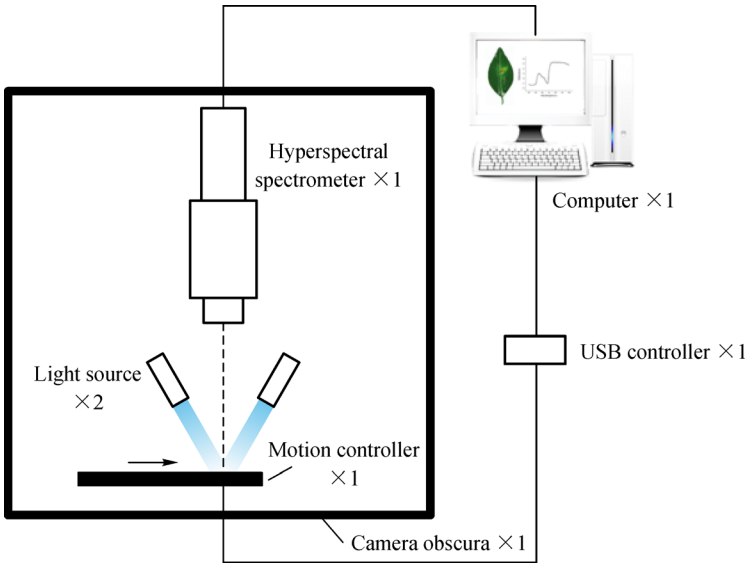

Fig. 1 Hyperspectral imaging system

where R is the relative reflection density of sample, R_S is the reflection density of the sample original image, R_W is the reflection density of white calibration image, R_D is the reflection density of dark calibration image.

2.3 PCR test

After the measurement of hyperspectral image, the leaf was tested by PCR Gene Amplification Instrument in the laboratory (Table 1). The leaf midrib was removed and the total DNA of the leaf was extracted using the CTAB (hexadecyltrimethylammonium bromide) method[21]. Then a standard PCR method was used to detect HLB bacteria of citrus[22]. The predicted PCR product from 16S rDNA amplification primers was 1167 bp, including:

OI_1: 5′GCGCGTATGCAATACGAGCGGCA3′;

OI_2: 3′GCCTCGCGACTTCGCAACCCAT5′.

After the reaction, 5 μL of PCR amplification and 10 × 1 μL of loading buffer with GelRed dye were mixed. The electrophoresis was conducted in 1% agarose gel and the result photographed with a gel imaging system. The positive lane was taken as the reference to determine whether the sample was infected with the HLB bacterium.

Table 1 The system and program of PCR reaction

20 μL reaction system	Program
10 × buffer, 2.0 μL	1st, pre-denaturation 94°C 5 min
10 mol·L^{-1} dNTP, 0.4 μL	2nd, denaturation 94°C 30 s
OI_1, 0.4 μL	3rd, primer annealing 60°C 30 s
OI_2, 0.4 μL	4th, extension 72°C 45 s
r*Taq*, 0.2 μL	35 cycles
DNA, 2.0 μL	5th, extension 72°C 10 min
H_2O, 14.6 μL	

3 Data processing

3.1 PCR testing results and data classification

Figure 2 shows the PCR electrophoresis pictures of representative samples. It was found that the leaf samples collected from the orchard without symptoms were negative, which meant that the trees were not infected with HLB. Of the leaves collected from the orchard with HLB symptoms, 93 samples were positive including 21 samples of normal color and 72 chlorotic leaves. The rest were negative. Since it is difficult to culture the HLB bacterium and the pathogenic bacteria are unevenly distributed in plant tissues, with low quantity and complexity in sample preparations, false negative results are sometimes found in PCR tests[23]. Therefore, this research used both PCR-positive and -negative leaves for modeling and predicting.

In the modeling analysis of spectral identification, 90 HLB-positive leaves from 93 PCR-positive samples and 90 HLB-negative leaves from PCR-negative orchard were selected randomly. The two groups contained 20 leaves with normal color and 70 chlorotic leaves. The grouping of the modeling set and the predicting set are shown in Table 2.

3.2 Spectral extraction and preprocessing

To eliminate background interference, HSI Analyzer software (Isuzu Optics Corp.) was used to separate the hyperspectral images, and the mask image of the leaf region was obtained as shown in Fig. 3. The average spectrum of white region, i.e., leaf region of citrus, was extracted as the spectral value of this leaf sample. To

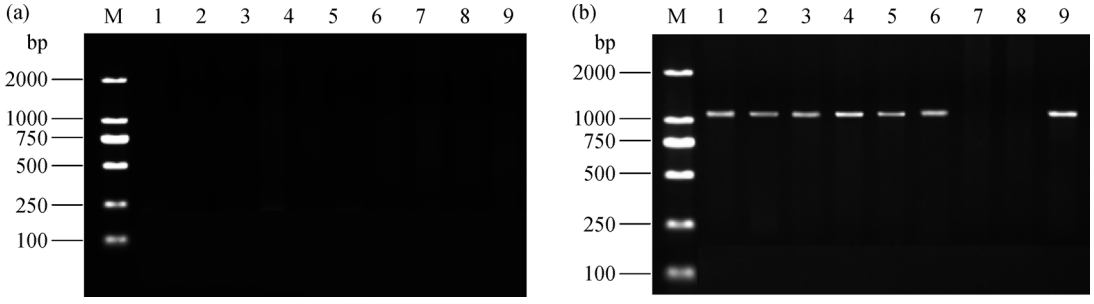

Fig. 2 Conventional PCR electrophoretogram of Newhall citrus leaf. (a) M, DL2000 marker; 1–9, nine leaf samples from HLB-free orchard; (b) M, DL2000 marker; 1–9, nine leaf samples from HLB-infected orchard.

Table 2 Grouping of leaf samples from HLB-free and-infected orchards

Group	HLB-free orchard			HLB-infected orchard		
	Calibration group	Validation group	Total	Calibration group	Validation group	Total
Normal color leaves	15	5	20	15	5	20
Chlorotic leaves	55	15	70	55	15	70
Total	70	20	90	70	20	90

eliminate influence from adverse factors, such as noise, baseline drift and shift, some algorithms such as 9-point smoothing, first-order derivative (D1), second-order derivative (D2), multiplicative signal correlation (MSC), standard normal variate (SNV) transformation, and others were adopted to preprocess the obtained leaf spectra.

3.3 Extraction of principal components

The principal components of the spectra from upper and lower leaf surfaces using different data pretreatments were extracted with Matlab® R2010a software (The Mathworks, Inc., Natick, MA, USA) and the cumulative contribution rate of the first N principal components was calculated. As shown in Fig. 4, when the number of principal components was 45, the cumulative contribution rate of principal components of different pretreated spectra all reached to 99%. Therefore, the first 45 principal components were selected as the input of the recognition model.

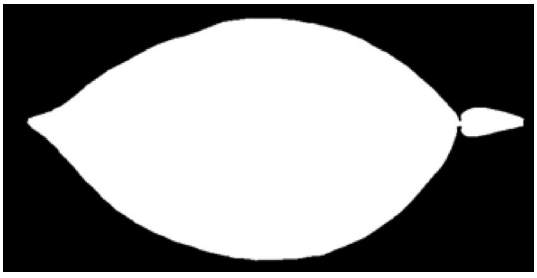

Fig. 3 Mask image of leaf region of citrus

3.4 Least squares support vector machine modeling analysis

The support vector machine (SVM) is a recent algorithm for machine learning. It has many advantages in solving practical problem, such as small sample set, nonlinear, high dimensional pattern and local minimum values[24]. The least squares support vector machine (LSSVM) is an improvement and expansion of traditional SVM, which adopts a structural risk minimization principle instead of empirical risk minimization principle. It has superior generalization ability and global optimalization and, compared with the forward neural network, it is not easy to over-fit. This research used Matlab® R2010a to establish the LSSVM discriminant model and adopted RBF kernel function $K(X_i,X_j) = \exp(-\gamma||X_i-X_j||)^2$ which had wide convergence domain.

4 Results and analysis

4.1 Spectral characteristics of leaf samples

It was observed from the original spectra of both upper and lower leaf surfaces that the variation trends of the spectral reflectance curves were similar and coincident with each other. Consequently, it was difficult to distinguish whether the leaves were infected with HLB or not. The spectral reflectance of leaf samples might be influenced by many factors, such as the growth condition, leaf structure and

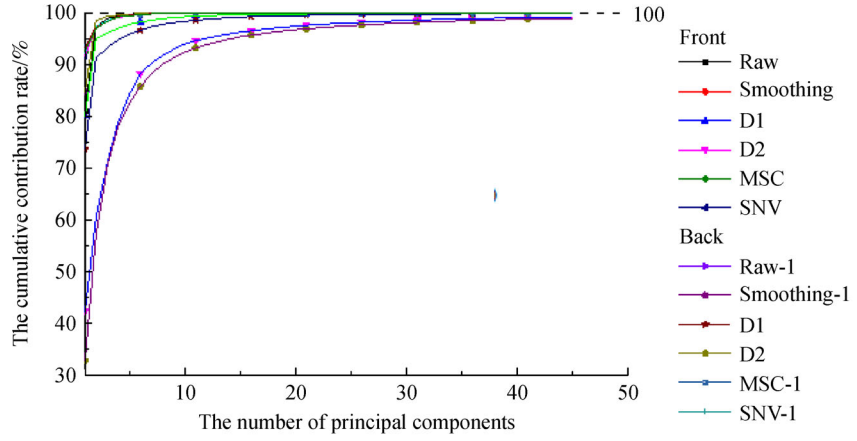

Fig. 4 The cumulative contribution rate of the principal components of the spectra from upper and lower leaf surfaces under different pretreatments. D1, First-order derivative; D2, second-order derivative; MSC, multiplicative signal correlation; SNV, standard normal variate.

constituents, the surrounding environment, and other factors. These factors can influence the external characteristics of leaf, such as color, texture and structure, and internal characteristics, such as chlorophyll, moisture and tissue composition, which results in some differences in spectral reflection characteristics of the leaf sample. Therefore, the difference in leaf spectral reflectance is not only caused by HLB infection, and it should be further analyzed using a chemometric method to extract the spectral information of the HLB-infected leaves.

The original average spectra of HLB-positive and -negative leaves from upper and lower surfaces are shown in Fig. 6. The curves have the typical NIR spectral characteristics of plant leaves. However, in the range of 400–700 nm the average spectral reflectance of the lower leaf surface was greater than that of the upper leaf surface, which might be attributed to higher content of chlorophyll in the upper surface, so that the leaves could absorb more solar radiation and reduce the spectral reflectance. It was observed that the average spectrum of HLB-positive leaves was higher than that of the HLB-negative leaves from both upper and lower surfaces, which showed that the leaf tissue infected with HLB had different spectral response characteristics.

4.2 Extraction of spectrum principal components

In this research, the scanned spectral range of Newhall citrus leaves was 400–1000 nm with 760 wavebands in total. Hyperspectral data contains large amount of information including redundant information, which goes against high-efficiency computational analysis. This research adopted Matlab to extract spectral principal components, which were treated as new variables. Those new variables had no correlation with each other and could represent most of the information contained in the original spectra. Figure 7 shows the score scattering of the top three principal components extracted from 140 modeling samples. The contribution rate of the top three components of upper leaf surface spectra were 81.0%, 16.5% and 1.5% (99.0% in total). Also, the contribution rate of the top three components of lower leaf surface spectra were 84.5%,

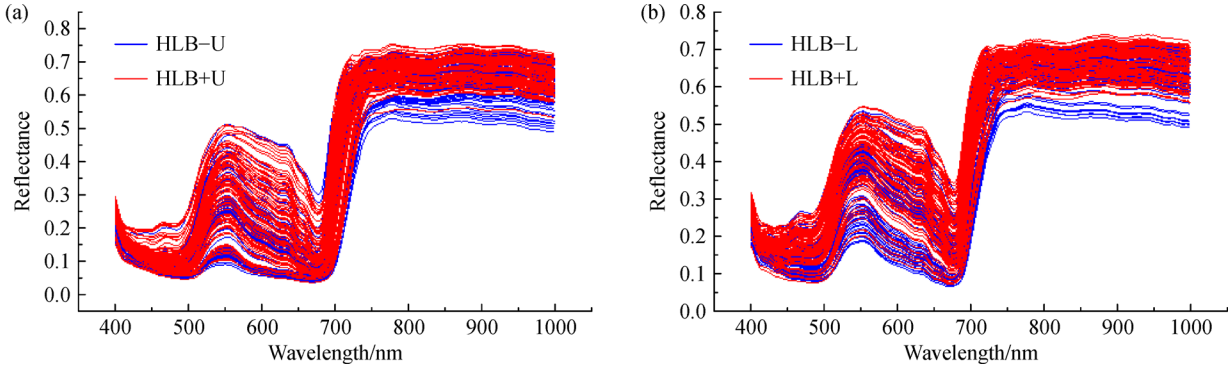

Fig. 5 Original spectra of leaf surfaces. (a) Upper; (b) lower. HLB + U, HLB positive upper; HLB + L, HLB positive lower; HLB–U, HLB negative upper; HLB–L, HLB negative lower.

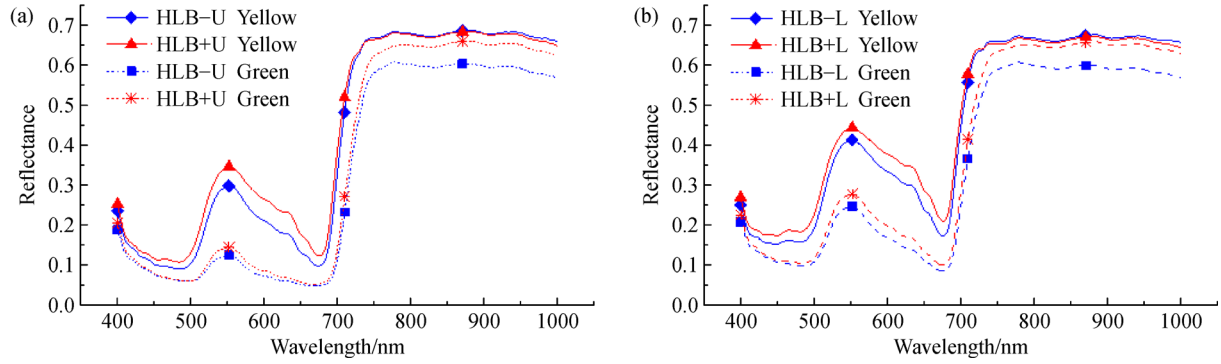

Fig. 6 Original average spectra of surfaces of HLB-negative and -positive citrus leaves. (a) Upper; (b) lower. HLB + U, HLB positive upper; HLB + L, HLB positive lower; HLB –U, HLB negative upper; HLB –L, HLB negative lower. Yellow and green are leaf color.

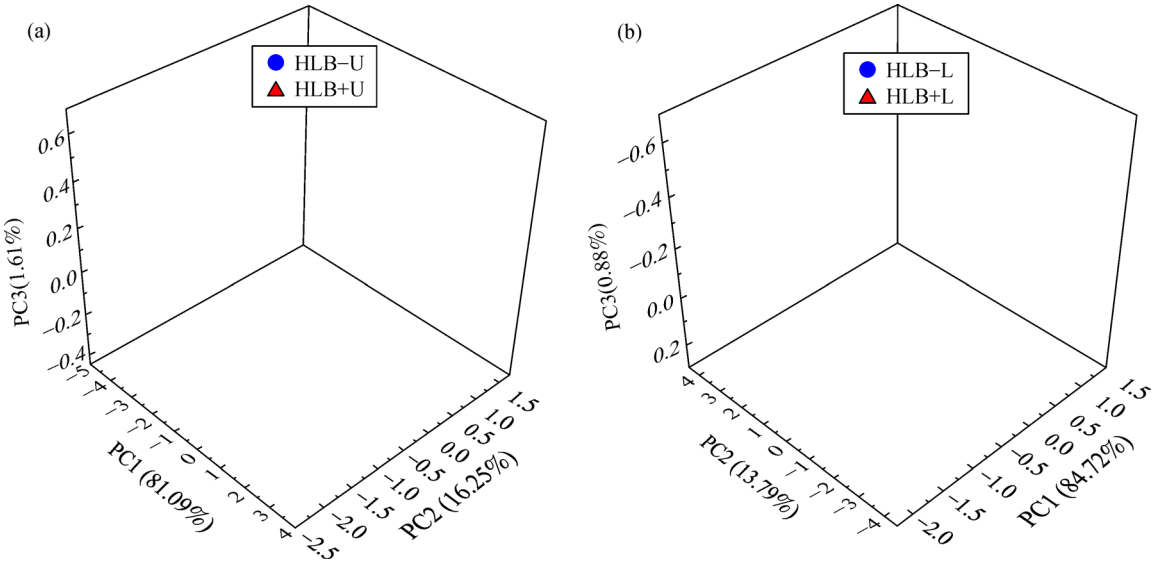

Fig. 7 3-D clustering chart of top three principal components extracted from leaf surface spectra of Newhall citrus. (a) Upper; (b) lower. HLB + U, HLB positive upper; HLB + L, HLB positive lower; HLB –U, HLB negative upper; HLB –L, HLB negative lower.

14.0%, and 1.0% (99.5% in total). From Fig. 7, it can be seen that it was difficult to distinguish HLB-negative and -positive leaves using principal component analysis directly. Hence, it is necessary to use the extracted principal components and perform further modeling computation.

4.3 Calibration and validation of LSSVM model

This study used the spectral data of 180 leaf samples to establish the LSSVM model for HLB disease identification. The samples were divided into two sets, 140 samples were used as the calibration set and the remaining 40 samples were used as the validation set. Since there were 760 wavebands in the 400–1000 nm range, the calibration data set was a matrix of 140 × 760 and the validation data set was a matrix of 40 × 760. The principal components were extracted from the original spectra and pretreated spectra such as 9-point smoothing, first-order derivative, second-order derivation, MSC, and SNV. Then different numbers of principal components were chosen for LSSVM modeling analysis. Based on the LSSVM model, the effects of the optimal principal components combined with each spectral preprocessing method on the modeling results were compared and analyzed and the results are shown in Table 3. The kernel function used by LSSVM was the RBF function, which had two important parameters, γ and σ^2. The combination of γ and σ^2 could determine the learning prediction ability of the LSSVM model, and the best combination was obtained by grid search and cross validation.

From Table 3 the highest recognition rate values of

Table 3 HLB identification models by least squares support vector machine model

Leaf surface	Preprocessing methods	γ	σ^2	Calibration data set			Validation data set		
				Number of samples	Recognition number	Recognition rate/%	Number of samples	Recognition number	Recognition rate/%
Upper	Original spectra	658.28	463.28	140	140	100.0	40	36	90.0
	9-point smoothing	599.70	249.04	140	140	100.0	40	37	92.5
	D1	0.30	325.40	140	138	98.5	40	34	85.0
	D2	1.90	160.30	140	140	100.0	40	36	90.0
	MSC	0.76	451.43	140	138	98.5	40	35	87.5
	SNV	0.75	511.31	140	138	98.5	40	33	82.5
Lower	Original spectra	0.20	225.05	140	137	98.0	40	36	90.0
	9-point smoothing	0.17	157.95	140	137	98.0	40	37	92.5
	D1	0.51	126.82	140	140	100.0	40	34	85.0
	D2	73.14	107.28	140	140	100.0	40	37	92.5
	MSC	35.78	845.29	140	140	100.0	40	36	90.0
	SNV	28.94	421.64	140	140	100.0	40	36	90.0

Note: D1, First-order derivative; D2, second-order derivative; MSC, multiplicative signal correlation; SNV, standard normal variate transformation.

calibration set and validation set were obtained for the upper leaf surface spectra obtained by 9-point smoothing pretreatment, which were 100% and 92.5% with the optimal γ and σ^2 of 599.70 and 249.04. While the highest recognition rate values based on lower leaf surface spectra under the second-order derivative pretreatment were also 100% and 92.5% with optimal γ and σ^2 of 73.14 and 107.28. The results showed that both the upper and lower leaf surface spectra contained useful information for recognizing HLB in Newhall citrus and could be used for identification of HLB.

The visible and NIR spectra in the range of 400–1000 nm can reflect the structure and biochemical components of leaf samples, such as chlorophyll and protein. The process of leaf infection with HLB is complicated, and the leaf structure and biochemical components will change. These changes would be expressed in the spectra used to identify infected leaves. The basis of the HLB disease identification model was the correlation between the spectrum and the changes of leaf constituents after infection rather than the direct relationship between the spectrum and the HLB bacterium.

Table 4 shows the precision evaluation confusion matrix of LSSVM models based on the spectra of upper and lower leaf surfaces. As shown from Table 4, for both upper and lower leaf surfaces spectra, 100% recognition rates of calibration sets for HLB-negative and -positive leaf samples were achieved. For LSSVM, the HLB recognition model based on the upper surface spectra with 9-point smoothing, three HLB samples were misjudged as HLB-negative samples in the validation set. A similar result was obtained from the model based on the lower surface spectra with second-order derivative. In general, the reason for the recognition error in the validation set was because the HLB-positive samples were mistaken for HLB-negative samples.

The best identification result was obtained from both the upper leaf surface model with 9-point smoothing pretreatment and the lower leaf surface model with D2 pretreatment. Table 5 shows classification results of unknown samples using the LSSVM model combined with the two pretreatment methods. False samples included two yellow samples, one normal leaf color, five normal color HLB-positive, with four correctly recognized. This illustrates that the high spectrum of citrus HLB early noninvasive diagnosis is possible, which can identify symptomless leaves infected with citrus HLB.

5 Conclusions

We used visible and NIR spectroscopy combined with an LSSVM algorithm to establish an identification model for HLB-negative and -positive Newhall orange leaves. Through the comparison and analysis of five different pretreatment methods, the best recognition result was obtained from the LSSVM model based on the upper leaf surface spectra after 9-point smoothing pretreatment. Further, the model established using the lower leaf surface spectra after D2 pretreatment achieved a better result. The determined calibration and validation sets all contained leaf samples with both normal color and different degrees of yellow. The calibration and validation results showed that the HLB-positive leaves whether of normal leaf color

Table 4 The precision evaluation confusion matrix of least squares support vector machine models based on the spectra of upper and lower leaf surfaces

Leaf surface	Pre-processing	Data set	Actual classification	Model classification		Recognition rate/%	Total recognition rate/%
				HLB-negative	HLB-positive		
Upper	9-point smoothing	Calibration	HLB-negative	70	0	100	100
			HLB-positive	0	70	100	
		Validation	HLB-negative	20	0	100	93
			HLB-positive	3	17	85	
Lower	D2	Calibration	HLB-negative	70	0	100	100
			HLB-positive	0	70	100	
		Validation	HLB-negative	20	0	100	93
			HLB-positive	3	17	85	

Note: D2, second-order derivative.

Table 5 Real categories and predicted categories results

Type of leaf	Upper surface spectra + 9-point smoothing				Lower surface spectra + SNV			
	Green		Yellow		Green		Yellow	
	Actual	Model	Actual	Model	Actual	Model	Actual	Model
Chlorotic	15	15	15	13	15	15	15	13
Normal color	5	5	5	4	5	5	5	4

or yellow were predicted correctly, which indicated that it was possible to use hyperspectral modeling to detect HLB disease even when chlorotic symptoms were absent. Only three misidentified samples were obtained, including two yellow color and one normal color samples. It can be concluded from this study that it is feasible to detect and predict Newhall citrus HLB using an LSSVM discriminant model established by the upper and lower leaf surface spectra measured by visible and NIR hyperspectral imaging technology. This method provided satisfactory prediction accuracy and laid the foundation for the real-time and nondestructive detection of citrus HLB disease.

Acknowledgements This work was supported by the 2011 Collaborative Innovation Center of the Southern Mountain Orchard Intelligent Management Technology and Equipment of Jiangxi Province (Jiangxi Finance Instruction No. 156 [2014]); the National Key R&D Program of China (2016YFD0200703).

Compliance with ethics guidelines Kejian Wang, Dongmei Guo, Yao Zhang, Lie Deng, Rangjin Xie, Qiang Lv, Shilai Yi, Yongqiang Zheng, Yanyan Ma, and Shaolan He declare that they have no conflicts of interest or financial conflicts to disclose.

This article does not contain any studies with human or animal subjects performed by any of the authors.

References

1. Yuan Y W, Ge L Q, Wang D P, Lin C Y. Influence of cruise HLB on the yield and quality. *Journal of Zhejiang Agricultural Sciences*, 2007, (1): 87–88 (in Chinese)
2. An H, Wang H G, Liu R Y, Cai C J, Ma Z H. Preliminary study on spectral characteristics of single leaf infected by *Puccinia striiformis*. *China Plant Protection*, 2006, **25**(11): 8–11 (in Chinese)
3. Qiao H B, Xia B, Ma X M, Cheng D F, Zhou Y L. Identification of damage by diseases and insect pests in winter wheat. *Journal of Triticeae Crops*, 2010, **30**(4): 770–774 (in Chinese)
4. Bo L, Liu Z Y, Huang J F, Zhang L L, Zhou W, Shi J J. Hyperspectral identification of rice diseases and pests based on principal component analysis and probabilistic neural network. *Transactions of the Chinese Society of Agricultural Engineering*, 2009, **25**(9): 143–147 (in Chinese)
5. Di W, Cao F, Zhang H, Sun G M, Feng L, He Y. Study on disease level classification of rice panicle blast based on visible and near infrared spectroscopy. *Spectroscopy and Spectral Analysis*, 2009, **29**(12): 3295–3299 (in Chinese)
6. Li J P, Chai A L, Shi Y X, Xie X W, Li B J. Early rapid detection of clubroot of Chinese cabbage using FTIR spectroscopy. *Spectroscopy and Spectral Analysis*, 2013, **33**(6): 1528–1531 (in Chinese)
7. Wu D, Zhu D S, He Y, Zhang C Q, Feng L. Nondestructive detection of grey mold of eggplant based on ground multi-spectral imaging sensor. *Spectroscopy and Spectral Analysis* 2008, **28**(7): 1496–1500 (in Chinese)
8. Feng L, Zhang D R, Chen S S, Feng B, Xie C Q, Chen Y Y. Early detection of gray mold on eggplant leaves using hyperspectral imaging technique. *Journal of Zhejiang University*, 2012, **38**(3): 311–317 (in Chinese)
9. Tian Y W, Li T L, Zhang L, Wang X J. Diagnosis method of cucumber disease with hyperspectral imaging in greenhouse. *Transactions of the Chinese Society of Agricultural Engineering*, 2010, **26**(5): 202–206 (in Chinese)

10. Feng L, Chen S S, Feng B, Liu F, He Y, Lou B G. Early detection of soybean pod anthracnose based on spectrum technology. *Transactions of the Chinese Society of Agricultural Engineering*, 2012, **28** (1): 139–144 (in Chinese)
11. Feng L, Chen S S, Feng B, Liu F, He Y, Lou B G. Spectral detection on disease severity of soybean pod anthracnose. *Transactions of the Chinese Society of Agricultural Machinery*, 2012, **43**(8): 175–179 (in Chinese)
12. Chen B, Wang K R, Li S K, Jin X L, Chen J L, Zhang D S. The effects of disease stress on spectra reflectance and chlorophyll fluorescence characteristics of cotton leaves. *Transactions of the Chinese Society of Agricultural Engineering*, 2011, **27**(9): 86–93 (in Chinese)
13. Chen B, Wang K R, Li S K, Jin X L, Chen J L, Zhang D S. Estimating severity level of cotton disease based on spectral indices of TM image. *Journal of Infrared and Millimeter Waves*, 2011, **30** (5): 451–457 (in Chinese)
14. Sankaran S, Mishra A, Maja J M, Ehsani R. Visible-near infrared spectroscopy for detection of Huanglongbing in citrus orchards. *Computers and Electronics in Agriculture*, 2011, **77**(2): 127–134
15. Mishra A, Ehsani R, Karimi D, Albrigo L G. Potential applications of multiband spectroscopy and hyperspectral imaging for detecting HLB infected orange trees. *Proceedings of the Annual Meeting of the Florida State Horticultural Society*, 2009, **122**: 147–151
16. Kumar A, Lee W S, Ehsani R J, Albrigo L G, Yang C, Mangan R L. Citrus greening disease detection using aerial hyperspectral and multispectral imaging techniques. *Journal of Applied Remote Sensing*, 2012, **6**(1): 063542
17. Mei H L, Deng X L, Hong T S, Luo X, Deng X L. Early detection and grading of citrus Huanglongbing using hyperspectral imaging technique. *Transactions of the Chinese Society of Agricultural Engineering*, 2014, **30**(9): 140–147 (in Chinese)
18. Deng X L, Kong C, Wu W B, Mei H L, Li Z. Detection of citrus Huanglongbing based on principal component analysis and back propagation neural network. *Acta Photonica Sinica*, 2014, **43**(4): 16–22 (in Chinese)
19. Deng X L, Zheng J B, Mei H L. Identification and classification of citrus Huanglongbing disease based on hyperspectral imaging. *Journal of Northwest A&F University (Natural Science Edition)*, 2013, **41**(7): 99–105 (in Chinese)
20. Tian X, He S L, Lü Q, Yi S L, Xie R J, Zheng Y Q, Liao Q H, Deng L. Determination of photosynthetic pigments in citrus leaves based on hyperspectral images datas. *Spectroscopy and Spectral Analysis*, 2014, **34**(9): 2506–2512 (in Chinese)
21. Gacher E, Martin G G. Detection of genetically modified organism (GMO) by PCR: a brief review of methodologies available. *Trends in Food Science & Technology*, 1999, **9**(11–12): 380–388
22. Jagoueix S, Bove J M, Garnier M. The phloem-limited bacterium of greening disease of citrus is a member of the alpha subdivision of the *Proteobacteria*. *Tnternational Journal of Systematic and Evolutionary Microbiology*, 1994, **44**(3): 379–386
23. Hu H, Yin Y, Zhang L. Detection of citrus Huanglongbing by conventional and two fluorescence quantitative PCR assays. *Scientia Agricultura Sinica*, 2006, **39**(12): 2491–2497 (in Chinese)
24. Yan W W, Zhu H D, Shao H H. Soft sensor modeling based on support vector machines. *Acta Simulata Systematica Sinica*, 2003, **15**(10): 1494–1496 (in Chinese)